Time-Resolved FT EPR and Optical Spectroscopy Study on Photooxidation of Aliphatic α-Amino Acids in Aqueous Solutions; Electron Transfer from Amino vs Carboxylate Functional Group

Peter Tarábek,[†] Marija Bonifačić,*[,‡] and Dieter Beckert*[,†]

Interdisciplinary Research Group "Time-Resolved Spectroscopy", Faculty of Chemistry and Mineralogy, University of Leipzig, Permoserstrasse 15, Leipzig, D-04318, Germany, and Department of Physical Chemistry, Ruđer Bošković Institute, Bijenička c. 54, HR-10 000 Zagreb, Croatia

Received: February 6, 2006; In Final Form: March 23, 2006

Using time-resolved Fourier transform electron paramagnetic resonance, FT EPR, and optical spectroscopy, the photooxidation of glycine, α-alanine, α-aminoisobutyric acid, and model compounds *β*-alanine, methylamine and sodium acetate, by excited triplets of anthraquinone-2,6-disulfonate dianion was studied in aqueous solutions in the pH range 5−13. Anthraquinone radical trianions showing strong emissive spin-polarization (CIDEP) were formed, indicating fast electron transfer from the quenchers to the spin-polarized quinone triplet as the primary reaction. None of the primary radicals formed upon one-electron oxidation of quenchers could be detected at the nanosecond time scale of FT EPR measurements because of their very fast transformation into secondary products. The latter were identified to be decarboxylated α-aminoalkyl radicals for α-amino acids anions and zwitterions, *β*-aminoalkyl radicals for *β*-alanine zwitterions, and methyl radicals for acetate anions; corresponding aminyl radicals were the first EPR detectable products from *β*-alanine anions and methylamine. Thus, anthraquinone-2,6-disulfonate triplet can take an electron from both NH_2- and $-CO_2^-$ functional groups forming aminium ($^{+\bullet}NH_2-$) and acyloxyl ($-CO_2^\bullet$) radicals, respectively. Aminium radicals derived from *β*-alanine anions and CH_3-NH_2 stabilize by deprotonation into aminyl radicals, whereas these derived from α-amino acids anions are known to suffer ultrafast decarboxylation ($\tau \sim 10$ ps). Analysis of the polarization patterns revealed that decarboxylation from acyloxyl radicals are considerably slower (ns $< \tau <$ 0.1 *μ*s). Therefore, in the case of α-amino acids, the isoelectronic structures $NH_2-CR_2-CO_2^\bullet$ and $^{+\bullet}NH_2-CR_2-CO_2^-$ probably do not constitute resonance mesomeric forms of one and the same species and the decarboxylation of aminium radicals is not preceded by the intramolecular carboxylate to amino group electron transfer. Absolute triplet quenching rate constants at zero ionic strength were in the range of 2×10^8 to 2×10^9 M^{-1} s^{-1} for $R-NH_2$ and 2×10^7 to 10^8 M^{-1} s^{-1} for $R-CO_2^-$ type of electron donors, reflecting in principle their standard reduction potentials. The strengths of acids: $^+NH_3-{}^\bullet CH_2$, $^+NH_3-{}^\bullet C(CH_3)H$, and $^+NH_3-{}^\bullet C(CH_3)_2$, p$K_a$ <4, >6, and >7, respectively, were found to be remarkably strongly dependent on α-C substitution. The conjugate bases of these α-aminoalkyl radicals reduce anthraquinone-2,6-disulfonate dianion ground state with $k_{sec} = 3 \times 10^9$ M^{-1} s^{-1}.

1. Introduction

In the last years a rapid increase of interest is observable in oxidative damage of proteins and its relevance to pathological disorders and aging (for recent reviews see, for example, refs 1−3). Amino acid side chains are very important sites of oxidation agents attack at proteins. Therefore, detailed investigations of reaction mechanisms and properties of amino acid and peptide derived radicals are imperative for better understanding of processes leading to the damage. Radicals of simple aliphatic α-amino acids and small peptides in aqueous solutions have been produced under various conditions and characterized by steady-state and time-resolved EPR and pulse radiolysis techniques, including initially produced radicals and these formed by the primary radicals subsequent reactions.[4−19] The main reactions and radical products of amino acid anions are exemplary shown for glycine in Scheme 1. The actual mechanism and the fraction of the three possible primary products, aminium radical zwitterion $^{+\bullet}NH_2-CH_2-CO_2^-$, aminyl radical anion $^\bullet NH-CH_2-CO_2^-$, and glycyl radical anion $NH_2-{}^\bullet CH-CO_2^-$, are dependent on the nature of the attacking species. The one-electron transfer from the nonbonding electron pair on the nitrogen under formation of $^{+\bullet}NH_2-CH_2-CO_2^-$ is a favorable mechanism for the reaction with excited molecules,[14,16] $SO_4^{\bullet-}$,[6] and hydroxyl radicals, the latter being also able to directly abstract H atom from N−H and C−H groups, Scheme 1, to an appreciable extent.[11;15;17;18] The aminium radical, which is isoelectronic with the acyloxyl radical $NH_2-CH_2-CO_2^\bullet$, was observed only in the X-ray irradiated single-crystal of glycine at low temperature[20;21] and was decomposing on warming by decarboxylation. In aqueous solutions, the decarboxylation, definitely the most dramatic consequence of an oxidative attack, occurs by an ultrafast rate constant of about 10^{11} s^{-1} [14] under formation of the reducing α-aminomethyl radical, $NH_2-{}^\bullet CH_2$. Deprotonation of the aminium radical to the aminyl form could be considered competitive with decarboxylation, at least for

* Corresponding authors. E-mail: (D.B.) beckert@mpgag.uni-leipzig.de; (M.B.) bonifacic@irb.hr.

[†] Interdisciplinary Research Group "Time-Resolved Spectroscopy", Faculty of Chemistry and Mineralogy, University of Leipzig.

[‡] Department of Physical Chemistry, Ruđer Bošković Institute.

10.1021/jp060764m CCC: $33.50
Published on Web 05/06/2006

SCHEME 1

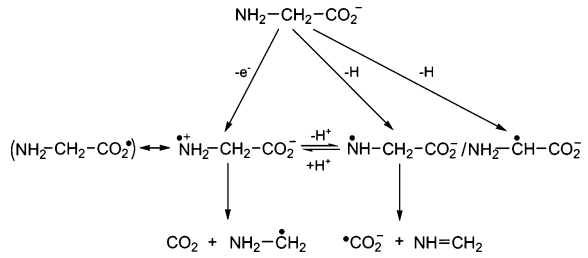

•OH as reactant, and, consequently, the strong base OH^- formation in close proximity, i.e., to take place within the solvent cage.[14,22] This is in opposite to the deprotonation from the much less acidic C−H position and formation of the reducing glycyl radical by the electron/proton-transfer mechanism.[22] Both aminyl and glycyl radicals could be pushed, however, into the fast decarboxylating aminium form in the presence of proton donors like phosphate buffer or glycine zwitterions.[11] This explained the observed production of CO_2 by a chain mechanism in the steady-state γ-radiolysis experiments, even under conditions where $^{\bullet}CH_3$ or $(CH_3)_2C^{\bullet}-OH$ radicals were employed as initiators. Thereby $NH_2-^{\bullet}CH_2$ radicals serve as the chain carrier, further producing glycyl radicals by H-abstraction from glycine anions.[11] Such secondary CO_2 production is an overall slow process occurring on approximately the millisecond time scale. Still another degradation reaction, namely a direct $^{\bullet}CO_2^-$ liberation from the aminyl radical, Scheme 1, is also relatively slow, $k \approx 10^3\ s^{-1}$.[13]

To take an electron or H atom from the α-amino acid zwitterions demands much higher energy[23] and, consequently, the rate constants for the oxidation reactions are considerably lower ($k(Gly^-)/k(Gly^{\pm}) = 2.9 \times 10^9/8.9 \times 10^6$ for •OH.[17] The only product identified with •OH as oxidant of the zwitterionic glycine has been $NH_2-^{\bullet}CH-CO_2H$,[5] but by using much stronger oxidation agent $SO_4^{\bullet-}$, the formation of the decarboxylated product $NH_2-^{\bullet}CH_2$ has been reported.[6] Decarboxylation occurs, however, with a high yield upon •OH radical oxidation of glycine in its basic anionic form.[9,11,15]

Our interest in the electron transfer reaction between photochemically generated anthraquinone-2,6-disulfonate dianion triplet (2,6-$AQDS_T$) and bioactive molecules[16,19,24−27] has prompted us to further investigate photoinduced oxidation of simple aliphatic α-amino acids anions and zwitterions in aqueous solution by FT EPR in the nanosecond time scale. For comparison, the oxidation of model compounds methylamine, acetate, and β-alanine have also been examined. Determination of the overall quenching rate constant of 2,6-$AQDS_T$ with all used electron donors have been measured by time-resolved optical spectroscopy. The results of studies we report here show that the strong oxidant 2,6-$AQDS_T$ can take an electron not only from $-NH_2$ but also from $-CO_2^-$ functional group. It results in generation of the respective aminium and acyloxyl radicals. These primary radicals could not be directly detected on the nanosecond time scale because of their very fast transformations into successor products which were identified by their characteristic FT EPR spectra.

The time-resolved Fourier transform electron paramagnetic resonance (FT EPR)[28−33] has been established as an appropriate method to investigate the structure and dynamic properties of short-lived free radicals and radical ions with high spectral resolution in the nanosecond and microsecond time scale. In most of these experiments, the paramagnetic species observed show strong spin polarization effects. Two CIDEP mechanisms,[34−36] the triplet mechanism[37,38] and the radical pair mechanism,[39−41] generate a nonthermal population of the doublet spin levels of the primary radical ions or neutral radicals. The triplet mechanism is described by the reaction sequence

$$A_{S0} \xrightarrow{308nm} A_{S1} \xrightarrow{ISC} A_T^* \xrightarrow{+D} \{A^{\bullet -*} \cdots D^{\bullet +*}\} \qquad (1)$$

where the first step is the excitation of the photosensitizer (A = anthraquinone-2,6-disulfonate in this study) by the laser pulse with photons of 308 nm, ISC denotes the intersystem crossing to the spin-polarized triplet state A_T^* and the last step is the electron transfer from the donor D to the acceptor triplet A_T^* (spin-polarized states are marked by *). This spin-polarized triplet state relaxes with the short spin−lattice relaxation time T_{1T} to the thermal equilibrium A_T in competition with the electron-transfer quenching of A_T^*. The quenching reaction transfers the spin polarization to the slower relaxing doublet radical ions $A^{\bullet -*}$ and $D^{\bullet +*}$ (or successor radicals of the chemically fast transforming $D^{\bullet +*}$ as it is the case with donors investigated in this study). Their EPR spectra are characterized by the strong emissive signals. Within the radical ion pair $\{A^{\bullet -*} \cdots D^{\bullet +*}\}$ the radical pair mechanism generates the radical pair polarization. The radical polarization induced by radical pair mechanism is generated by the processes of $S-T_0$-mixing of the radical pair states, the exchange interaction at closed approach of the pair and the reencounter of geminate radicals.[41] Radical pair polarization is mostly characterized by the E/A polarization pattern. In the case of the anthraquinone-2,6-disulfonate radical anion spectrum, the contribution of radical pair polarization can be neglected.

Using 2,6-AQDS as the photosensitizer has several advantages: its high extinction coefficient at 308 nm[42] and high quantum yield for the triplet formation[43] allow one to perform experiments in the presence of relatively low 2,6-AQDS concentration (0.2−1 mM applied in this study). This slows down the possible reaction of an electron donor derived radical having reducing properties with 2,6-AQDS ground state ($E°$-(2,6-AQDS/2,6-$AQDS^{\bullet -}$) = −0.31 V[44]), thus allowing such reductive radicals detection also on a microsecond time scale. Furthermore, the 2,6-AQDS triplet is a strongly one-electron oxidizing agent with a standard reduction potential of 2.37 V[44] and is therefore efficiently quenched by many electron donors. The resulting radical anion 2,6-$AQDS^{\bullet -}$ is a highly stabilized, long living radical decaying in the millisecond time scale and has, due to the small hyperfine coupling constants,[45] a narrow EPR spectrum which does not significantly overlap with the lines of other radicals. This spectrum has been used as an internal standard to determine the g-factor of unknown radicals.

2. Experimental Section

The 308 nm XeCl line of an excimer laser (Lambda Physik, LPX 105 ESC; energy 10−30 mJ per pulse; pulse width 16 ns) was used for photoexcitation in FT EPR experiments. The FT EPR equipment has been described previously.[42,45,46] The power of the microwave pulse used in the experiments was 1 kW with a pulse length for the $\pi/2$ pulse of 16 ns. The excitation width in the spectra was thus about $\Delta B = \pm 1.5$ mT. The cavity was the Bruker splitring module ER 4118X-MS-5W. The receiver dead time was on the order of 80−100 ns. All experimental FID data were extrapolated using the linear prediction singular value decomposition method (LPSVD).[42,47]

In the time-resolved optical experiments solutions were photolyzed by the third harmonic (355 nm) of a Quanta-Ray GCR-11 Nd:YAG laser (Spectra Physics). Pulses of ≤3 ns

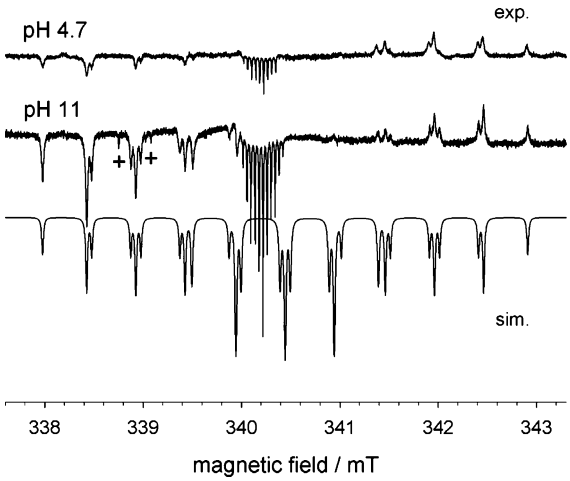

Figure 1. Experimental and simulated FT EPR spectra of the α-aminomethyl radical $NH_2-{}^{\bullet}CH_2$. Sample: 0.3 mM 2,6-AQDS and 1 M glycine (pH 4.7) or 0.1 M glycine (pH 11) in aqueous solution; delay 96 ns. Lines denoted by + belong to the radical $NH_2-{}^{\bullet}CH-CO_2^-$ with a yield ≤5%. The spectra of 2,6-AQDS$^{\bullet-}$ (central lines groups) are multiplied by 0.25.

duration (fwhm) with energies of up to 5 mJ were used. The optical detection system consisted of a pulsed xenon lamp (XBO 450, Osram), a monochromator (SpectraPro 275, Acton Research), a R955 photomultiplier tube (Hamamtsu Photonics), and a 500 MHz digitizing oscilloscope (DSA 602 A, Tektronix). The laser power was monitored for every pulse using a bypass with a fast Si-photodiode.

Anthraquinone-2,6-disulfonic disodium salt (2,6-AQDS, Aldrich), amino acids (Fluka), methylamine (Acros), and sodium acetate (Sigma) were used without further purification. Water was taken from a milli-Q plus ultrapure water system (Millipore). Deuterium oxide (99.8%) from Deuchem GmbH (Leipzig) was used for measurements with D_2O as a solvent. The solution flowed through the EPR tube (optical path length about 1.0 mm) at a rate of about 10 mL/min to avoid depletion of the sensitizer and/or enrichment of reaction products. The double-sided glass tube system before the resonator allows the sample temperature to be varied (for aqueous systems between 5 and 80 °C). KOH and $HClO_4$ (Aldrich) were used to adjust the pH. To remove oxygen, the samples were bubbled with argon (99.99%) before (about 20 min) and during the whole experiment. All measurements were carried out at room temperature.

3. Results

3.1. Glycine as Electron Donor. The complete FT EPR spectra obtained in aqueous solutions containing 0.3 mM 2,6-AQDS and 0.1 M glycine at pH 11 (96% in anionic form, $NH_2CH_2CO_2^-$) or 1 M glycine at pH 4.7 (only zwitterionic form present, $^+NH_3CH_2CO_2^-$) at a delay time of 96 ns between the laser and the microwave detection pulses are shown in Figure 1. The central lines groups belong to the radical anion 2,6-AQDS$^{\bullet-*}$.[45,48] At both pHs, the radical anion part of the spectrum shows an emissive behavior which is caused by the fast electron transfer from the donor glycine to the emissive polarized 2,6-AQDS triplet. Thereby the strength of polarization is proportional to the rate of the electron transfer reaction. The spectrum at pH 11 is stronger emissive polarized than the spectrum at pH 4.7 despite 10 times higher donor concentration in the acidic solution. This indicates a much faster electron transfer under basic conditions (for more details, see below). The E/A polarized line groups are due to the successor radical of the primary glycine radicals formed upon reductive quenching of 2,6-AQDS triplets. Because of the short lifetimes, these primary glycine radicals are undetectable by our FT EPR setup. The spectra, and therefore the structures of the successor radicals, are identical at both pH values considered and can unambiguously be assigned to the α-aminomethyl radical $NH_2-{}^{\bullet}CH_2$.[16] The hfs coupling constants determined by the spectra simulation are in very good agreement with earlier published data[4,16] and are collected in Table 1. From this we conclude that the amino group of $NH_2-{}^{\bullet}CH_2$ at pH 4.7 is still not protonated and, therefore, the pK_a value of equilibrium (2)

$$^+NH_3-{}^{\bullet}CH_2 \rightleftharpoons NH_2-{}^{\bullet}CH_2 + H^+ \qquad (2)$$

is below 4 (in comparison: pK_a($^+NH_3-$R) = 10.65 for methylamine and 9.6 for glycine). The only but essential difference of the FT EPR spectra of the successor radical $NH_2-{}^{\bullet}CH_2$ at pH 4.7 and 11 lies in their polarization behavior. Whereas at pH 11 the low field line groups show more emissive intensity than the high field line groups absorptive intensity (E*/A spectrum) due to the triplet polarization contribution, the spectrum at pH 4.7 is of pure E/A character independent of the donor concentration. This result gives some indication about the nature of the different precursors of $NH_2-{}^{\bullet}CH_2$ at pH 11 and 4.7, respectively (see Discussion). In the basic solution spectrum some small additional lines (signed by +) were observed. These lines belong to the glycyl radical $NH_2-{}^{\bullet}CH-CO_2^-$ as it has been shown earlier.[4,16] The yield of this radical is, however, low and amounts to ≤5% of the α-aminomethyl radical.

3.2. α-Alanine as Electron Donor. With α-alanine as an electron donor the same experiments were done as with glycine, Figures 2 and 3. Figure 2 shows the low field FT EPR spectra obtained with 0.3 mM 2,6-AQDS and 0.1 M α-alanine (pH 11) or 1 M α-alanine (pH 5) in aqueous solutions at the delay time of 96 ns. The polarization of the radical anion 2,6-AQDS$^{\bullet-*}$ shows behavior similar to that with glycine (strong emissive intensity at pH 11 and a smaller one at pH 5), which indicates similar reaction mechanisms and efficiencies for the primary electron-transfer processes. However, here we observe that the structures of the primary oxidized α-alanine successor radicals differ depending on pH. The hfs coupling constants for both radicals were determined by simulations and the structures could be assigned to the radical $NH_2-{}^{\bullet}CH(CH_3)$[16] at pH 11 and its protonated form $^+NH_3-{}^{\bullet}CH(CH_3)$ at pH 5. The protonation state at pH 5 was unambiguously proven by an experiment in D_2O (see Figure 3). The obtained hfs coupling constants are listed in Table 1. It is interesting that whereas with glycine the protonation state of the corresponding α-aminoalkyl radical is the same at both pH values, with α-alanine this is not the case. The results indicate that the pK_a value of $^+NH_3-{}^{\bullet}CH(CH_3)$ has to be ≥6, i.e., at least two pH units higher than that of $^+NH_3-{}^{\bullet}CH_2$ and, therefore, closer to its parent compound α-alanine (pK_a($^+NH_3-$R) = 9.69) in comparison to glycine. Again, similar to glycine, there is an essential difference in the polarization pattern between $^+NH_3-{}^{\bullet}CH(CH_3)$ and $NH_2-{}^{\bullet}CH(CH_3)$: under basic conditions where $NH_2-{}^{\bullet}CH(CH_3)$ radical dominates the contribution of triplet polarization is larger than under acidic conditions. In the spectrum of basic solution some small additional lines (marked by +) were observed. These lines belong to the alanyl radical $NH_2-{}^{\bullet}C(CH_3)-CO_2^-$ which has been checked by a simulation with parameters from ref 4; see also ref 16. Again, the yield of this radical is low, only ≤5% of the α-aminoalkyl $NH_2-{}^{\bullet}CH(CH_3)$.

3.3. α-Aminoisobutyric Acid as Electron Donor. The experiments with α-aminoisobutyric acid as an electron donor

TABLE 1: Hyperfine Coupling Constants A (in mT) and *g*-Factors for the Radicals Derived from Amino Acids[a]

donor	radical	*A*(**N**)/mT	*A*(**H**-N)/mT	*A*(**H**-C)/mT	*A*(C**H**$_3$)	*g* value	ref
Gly$^-$	$NH_2-{}^\bullet CH_2$	0.500	0.448 (2)	1.518 (2)		2.00289	
	$NH_2-{}^\bullet CH-CO_2^-$	0.610	0.339; 0.290	1.369		2.00347	16
Ala$^-$	$NH_2-{}^\bullet C(CH_3)H$	0.325	0.645 (2)	1.466	2.105 (3)	2.00300	16
	$NH_2-{}^\bullet C(CH_3)-CO_2^-$	0.507	0.193; <0.02		1.386 (3)	2.00334	4
Ala$^\pm$	$^+NH_3-{}^\bullet C(CH_3)H$	0.33	1.75 (3)	2.27	2.67 (3)	2.00251	
	$^+ND_3-{}^\bullet C(CH_3)H$	0.329	0.265 (3)	2.27	2.68 (3)	2.00273	
α-MeAla$^-$	$NH_2-{}^\bullet C(CH_3)_2$	0.130	0.599 (2)		1.879 (6)	2.00295	16
α-MeAla$^\pm$	$^+NH_3-{}^\bullet C(CH_3)_2$	0.286	1.59 (3)		2.43 (6)	2.00271	
β-Ala$^-$	$^\bullet NH-(CH_2)_2-CO_2^-$	1.367	2.28	4.17 (1*β*) 4.22 (1*β*)		2.0044	
β-Ala$^\pm$	$^+NH_3/NH_2-CH_2-{}^\bullet CH_2$	0.514	n.d.	2.249 (2α) 2.625 (2*β*)		2.002 63	

[a] In parentheses, the number of equivalent protons is shown. α-MeAla = α-aminoisobutiric acid; n.d. = not determined.

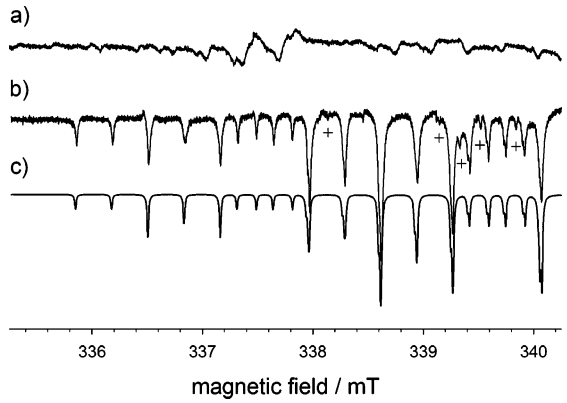

Figure 2. Low field parts of the FT EPR spectra obtained with α-alanine as electron donor. Samples: (a) 0.3 mM 2,6-AQDS, 1 M α-alanine (pH 5.0), delay 96 ns; (b) 0.3 mM 2,6-AQDS, 0.1 M α-alanine (pH 11), delay 96 ns; (c) simulated spectrum of the radical $NH_2-{}^\bullet C(CH_3)H$ with the parameters given by Lü et al.[16] Lines denoted by + belong to the radical $NH_2-(CH_3)C^\bullet-CO_2^-$.

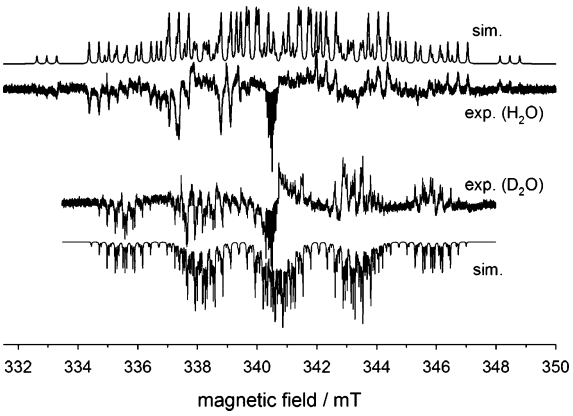

Figure 3. Experimental and simulated FT EPR spectra obtained with α-alanine as electron donor at the delay of 96 ns. Samples: 1 mM 2,6-AQDS and 1 M α-alanine in H_2O and in D_2O at pH 5.0 (pD 5.4). The simulation parameters are listed in Table 1. The spectra of 2,6-AQDS$^{\bullet-}$ (central lines groups) are multiplied by 0.05 (H_2O) and 0.1 (D_2O).

in basic solution amounted in similar results as obtained with α-alanine.[16] The FT EPR spectrum with 1 mM 2,6-AQDS and 0.5 M α-aminoisobutyric acid at pH 6 is depicted in Figure 4. The hfs coupling constants obtained by simulation are listed in Table 1 and are assigned to the radical structures $NH_2-{}^\bullet C(CH_3)_2$ at pH 11 (spectrum not shown here, see ref.[16]) and $^+NH_3-{}^\bullet C(CH_3)_2$ at pH 6. This again means that the pK_a value of $^+NH_3-{}^\bullet C(CH_3)_2$ (pK_a > 7) is much closer to the one of the parent compound α-aminoisobutyric acid (pK_a($^+NH_3-$R) = 10.19) in comparison with the couple $^+NH_3-{}^\bullet CH_2$/glycine. Concerning

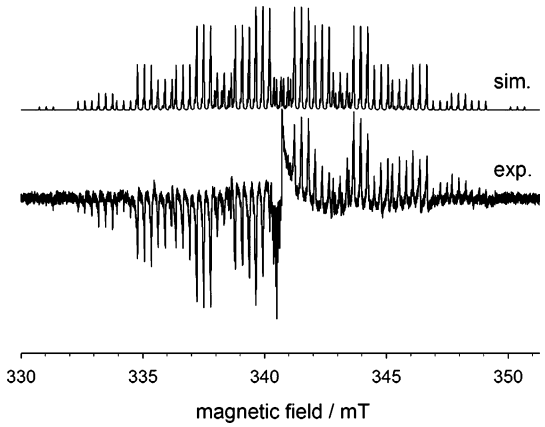

Figure 4. Experimental and simulated FT EPR spectra obtained with α-aminoisobutyric acid zwitterion as electron donor at the delay of 96 ns. Sample: 1 mM 2,6-AQDS and 0.5 M α-aminoisobutyric acid zwitterion at pH 6. The simulation parameters are listed in Table 1. The spectrum of 2,6-AQDS$^{\bullet-}$ (central lines groups) is multiplied by 0.1.

the polarization pattern, the results are similar to glycine and α-alanine.

3.4. *β*-Alanine, Methylamine and Acetate Ion as Model Compounds for α-Amino Acid Functional Groups. To support the interpretation that the 2,6-AQDS triplet not only can oxidize α-amino acids at NH_2- but also can take an electron from $-CO_2^-$ terminal groups, some experiments with *β*-alanine, methylamine, and sodium acetate as electron donors were carried out.

By insertion of an additional $-CH_2-$ group between the terminal amino and $-CO_2^-$ groups of glycine the electronic correlation between these terminal groups is decoupled and one should, therefore, expect different oxidation products of *β*-alanine under basic and acidic conditions. The respective FT EPR spectra of 0.5 mM 2,6-AQDS and 0.1 M *β*-alanine (pH 13) or 0.2 M *β*-alanine (pH 6.9) solutions are shown in Figures 5 and 6. The hfs coupling constants obtained by simulation are listed in Table 1. In basic solution these parameters are assigned to the aminyl radical $^\bullet NH-CH_2-CH_2-CO_2^-$ and in neutral solution to *β*-aminoethyl radical $^+NH_3-CH_2-{}^\bullet CH_2$ or its deprotonated form $NH_2-CH_2-{}^\bullet CH_2$. The two protonation forms of the carbon-centered radical could not be distinguished because the hfs coupling of the NH protons is unresolved. In the FT EPR spectrum of basic solution additional lines (marked by +) were observed. These lines belong to an incomplete spectrum because some lines overlap with lines belonging to the aminyl radical $^\bullet NH-CH_2-CH_2-CO_2^-$ and some lines are canceled by polarization effects. Therefore, a simulation of the spectrum and also an estimation of the relative yield were not possible.

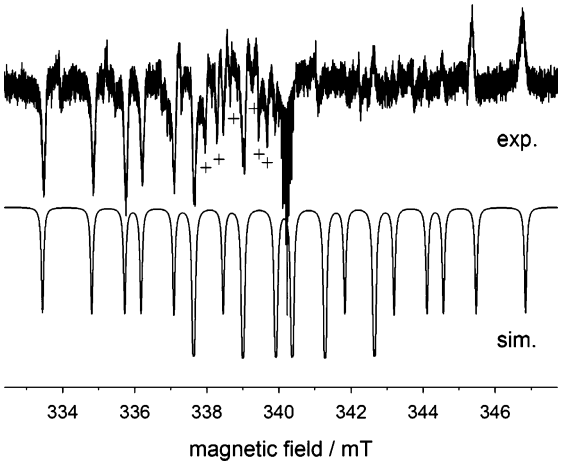

Figure 5. Experimentally obtained and simulated FT EPR spectra of the aminyl radical $^{\bullet}NH-(CH_2)_2-CO_2^-$. Sample: 0.5 mM 2,6-AQDS with 100 mM *β*-alanine at pH 13, delay 96 ns. The simulation parameters are listed in Table 1. The lines of the anion radical 2,6-AQDS$^{\bullet-}$ spectrum are multiplied by 0.05. For lines denoted by +, see text.

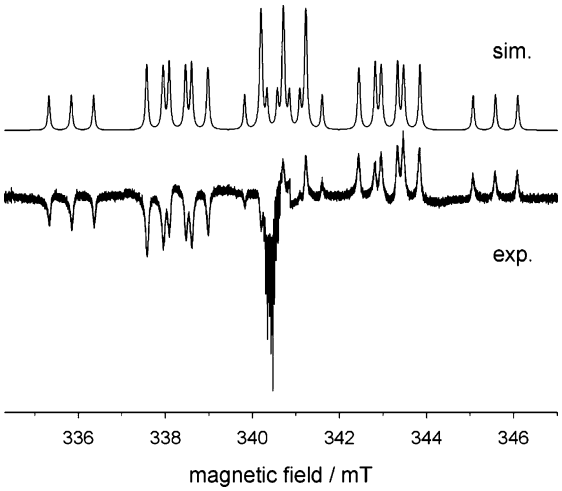

Figure 6. Experimental and simulated FT EPR spectra of the radical $^{+}NH_3/NH_2-CH_2-^{\bullet}CH_2$. Sample: 0.5 mM 2,6-AQDS, 200 mM *β*-alanine, pH 6.9, delay 96 ns. The simulation parameters are listed in Table 1. The lines of the anion radical 2,6-AQDS$^{\bullet-}$ spectrum are multiplied by 0.05.

However, this incomplete spectrum is most probably due to the radical $NH_2-^{\bullet}CH-CH_2-CO_2^-$. Similar to the observation in systems with α-amino acids, the polarization behavior of *β*-alanine derived radicals in the basic solution is of E*/A nature and a pure E/A pattern exists at neutral pH.

The FT EPR spectrum with methylamine at pH 13 as electron donor (Figure 7) consists of two subspectra (in addition to the anthraquinone radical anion spectrum) where the spectrum with stronger intensity can be unambiguously assigned to the aminyl radical $^{\bullet}NH-CH_3$ and the lines marked by (+) belong to the α-aminomethyl radical $NH_2-^{\bullet}CH_2$. The relative yield of $NH_2-^{\bullet}CH_2$ in comparison to $^{\bullet}NH-CH_3$ is up to 20%. The simulation parameters for the aminyl radical agree with the values given by Symons.[49] The line positions of the α-aminomethyl radical $NH_2-^{\bullet}CH_2$ are identical to those of the radical detected with glycine (Figure 1). Both radicals show similar ratios of triplet to radical pair polarization with (E*/A) patterns.

Photooxidation of the carboxyl group was studied by using the model compound sodium acetate as an electron donor. In Figure 8, the FT EPR spectrum is shown, which has been obtained in the solution with 0.5 mM 2,6-AQDS, 0.2 M acetate

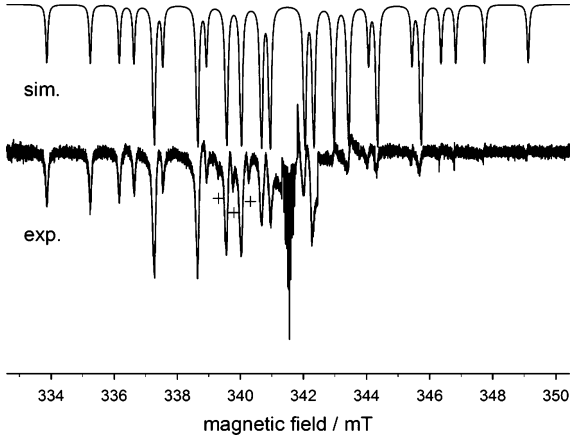

Figure 7. Experimental and simulated FT EPR spectra of the radical $^{\bullet}NH-CH_3$. Sample: 1 mM 2,6-AQDS, 100 mM CH_3NH_2 at pH 13, delay 96 ns. The simulation parameters ($3 \times A(\mathbf{H}-C) = 3.400$ mT, $A(N\mathbf{H}) = 2.298$ mT and $A(\mathbf{N}H) = 1.381$ mT, $g = 2.00427$) are in good agreement with the results from Symons.[49] The lines of the anion radical 2,6-AQDS$^{\bullet-}$ spectrum are multiplied by 0.05. Lines denoted by (+) belong to the radical $NH_2-^{\bullet}CH_2$.

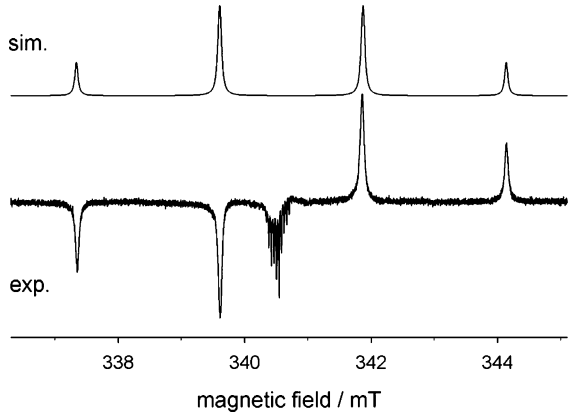

Figure 8. Experimental and simulated FT EPR spectra of the methyl radical $^{\bullet}CH_3$. Sample: 0.5 mM 2,6-AQDS, 200 mM CH_3COONa at pH 9.4, delay 96 ns. The simulation parameters ($3 \times A(\mathbf{H}\text{-}C) = 2.262$ mT, $g = 2.00288$) are in good agreement with the results from the literature.[50]

at pH 9.4 and at a delay of 96 ns. The only products observed were the radical anion 2,6-AQDS$^{\bullet-}$ and the methyl radical, $^{\bullet}CH_3$, showing a small triplet polarization (2,6-AQDS$^{\bullet-}$) and a pure radical pair polarization, the E/A pattern ($^{\bullet}CH_3$).

3.5. Triplet Deactivation Kinetics Measured by Time-Resolved Optical Spectroscopy. The transient optical absorption spectrum of the triplet state of 2,6-AQDS possesses a maximum at 380 nm.[44,50,51] After a pulse excitation of 2,6-AQDS containing solutions with the third harmonic of the Nd:YAG laser (355 nm) the decay kinetics of the 2,6-AQDS triplet at 380 nm was measured as a function of different electron donors concentration. Under our experimental conditions (oxygen free aqueous solutions containing 0.2 mM 2,6-AQDS, pH range 5−11), the lifetime of 2,6-AQDS$_T$ in the absence of any donor was 0.75 ± 0.12 *μ*s and was not altered by addition of up to 0.1 M $NaClO_4$. The triplet decay kinetics was always exponential and accelerated in the presence of donors (at least four different donor concentrations were used for each rate constant determination). To keep a quencher in the desired protonation form measurements were done at a constant pH away enough from the compound's pK_a value but not above pH 11. This assured that the contribution of the other protonation form(s) of the same quencher and/or OH^- present in the system

TABLE 2: Rate Constants for Quenching of 2,6-AQDS Triplet by Different Electron Donors in Aqueous Solutions[d]

donor	pK_a	pH	k_q[a]	$k_{q,0}$[b]
$NH_2-CH_2-CO_2^-$ **(Gly$^-$)**	2.34; 9.6	10.5	15 ± 2[c]	4.9 ± 0.6
$NH_2-CH(CH_3)-CO_2^-$ **(Ala$^-$)**	2.35; 9.69	10.5	15 ± 2[c]	4.9 ± 0.6
$NH_2-CH_2-CH_2-CO_2^-$ **(β-Ala$^-$)**	3.6; 10.19	10.2	7.7 ± 0.2[c]	2.5 ± 0.1
$CH_3-CO_2^-$	4.75	9.7	1.36 ± 0.03[c]	0.44 ± 0.01
$^+NH_3-CH_2-CO_2^-$ **(Gly$^\pm$)**	2.34; 9.6	5.2	0.16 ± 0.01	0.16 ± 0.01
$^+NH_3-CH(CH_3)-CO_2^-$ **(Ala$^\pm$)**	2.35; 9.69	5.4	0.32 ± 0.01	0.32 ± 0.01
$^+NH_3-CH_2-CH_2-CO_2^-$ **(β-Ala$^\pm$)**	3.6; 10.19	5.7	1.15 ± 0.04	1.15 ± 0.04
NH_2-CH_3	10.62	10.8	18.7 ± 0.7	18.7 ± 0.7
OH$^-$			5.0 ± 0.2[c]	1.61 ± 0.06

[a] Measured overall rate constants, [2,6-AQDS] = 0.2 mM. [b] Corrected quenching rate constants to zero ionic strength for charged electron donors (see text). [c] Measured at constant ionic strength $I = 0.1$ M. [d] Units: 10^8 M^{-1} s^{-1}.

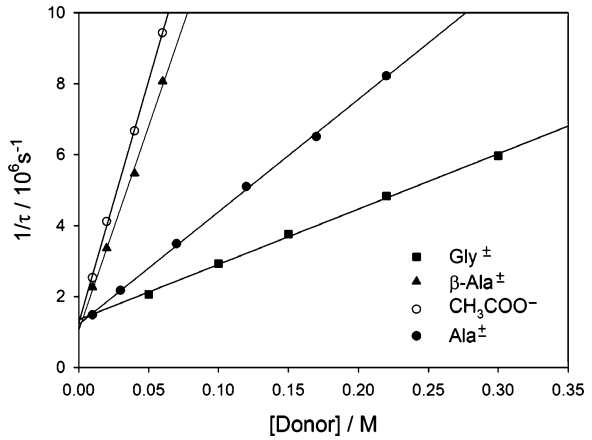

Figure 9. Decay rates of 2,6-AQDS triplet determined by time-resolved optical spectroscopy (380 nm) vs electron donors concentration. Samples: 0.2 mM 2,6-AQDS, pH ~ 6 for zwitterionic molecules and pH ~ 10, $I = 0.1$ M (adjusted by $NaClO_4$) for acetate.

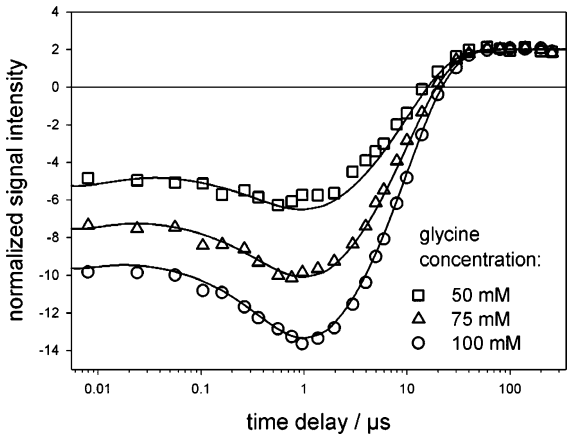

Figure 10. FT EPR time profiles of 2,6-AQDS$^{\bullet-}$ normalized signal intensity obtained at different glycine concentrations. Samples: 0.5 mM 2,6-AQDS, pH 12 and ionic strength $I = 0.1$ M (adjusted with $NaClO_4$).

to the overall quenching process was negligible (for pHs of specific measurements and donor pK_a values see Table 2). Only the concentration of a donor in the desired protonation form was used for the specific rate constant calculation. Since pK_{a1} < 3 for 2,6-AQDS ground state,[44] it has been considered that its triplet was also in the dianion form in all systems. Thus, for several donors used the interaction with 2,6-AQDS$_T$ refers to the reaction between electrically charged species for which the kinetic salt effect has to be taken into account. Such systems were measured at a constant ionic strength of $I = 0.1$ M adjusted by appropriate amount of $NaClO_4$, an inert salt concerning the triplet quenching. It has been assumed that the rate constants for zwitterionic quenchers are not sensitive to the presence of ions in the solution. The experimentally obtained second-order rate constants for the triplet deactivation by selected electron donors were determined from the slopes of the respective Stern−Volmer plots (Figure 9) and are listed in Table 2 as k_q values (error limits whenever given in this paper refer only to the least-squares fits of the experimental data). Values at zero ionic strength for electrically charged quenchers were calculated according to the Brönstedt−Bjerrum equation and are given as $k_{q,0}$ values in Table 2.[52] Intercepts of the straight lines obtained (Figure 9) were in very good agreement with the decay rate constant of 2,6-AQDS$_T$ measured in the absence of electron donors and also to the values reported earlier for 2,6-AQDS$_T$ deactivation rate in water.[53]

Because in the course of this work a number of experiments had to be done at elevated pH, care was taken to avoid participation of OH^- ions in the overall quenching process. From the measurements at constant $I = 0.1$ M, the rate constant at zero ionic strength $k_{q,0}(OH^-) = 1.61 \times 10^8$ M^{-1} s^{-1} [52] was calculated (Table 2). This value has been used as a base for checking possible OH^- involvement in other systems.

3.6. Secondary Reduction of 2,6-AQDS by α-Aminoalkyl Radicals—Time Profiles of 2,6-AQDS$^{\bullet-*}$ FT EPR Signal Intensities for Gly$^-$ as Quencher. The time profiles of 2,6-AQDS$^{\bullet-}$ normalized signal intensities measured with three different glycine concentrations, at constant [2,6-AQDS] = 0.5 mM, pH 12, and $I = 0.1$ M are shown in Figure 10 in the range of 10 ns to 300 μs. These time profiles are influenced by the primary electron-transfer process, k_q[Gly$^-$], accompanied by a strong triplet polarization transfer. The latter is in competition with the spin−lattice relaxation of 2,6-AQDS$_T$*. These processes are finished on ~10 ns time scale. Further increase of the emissive signal intensities on 0.1−1 μs is ascribed to the formation of 2,6-AQDS$^{\bullet-*}$ in a secondary electron-transfer reaction. Namely, as shown above, α-aminoalkyl radicals are practically the only products formed upon 2,6-AQDS$_T$ oxidation of α-amino acids. These radicals are strongly reducing and should be able to efficiently transfer an electron to 2,6-AQDS ground state, eq 3 ($E°$(2,6-AQDS/2,6-AQDS$^{\bullet-}$) = −0.31 V).[44,54]

$$\text{2,6-AQDS} + NH_2-{}^{\bullet}CH_2 \xrightarrow{k_{sec}} \text{2,6-AQDS}^{\bullet-} + NH{=}CH_2 + H^+ \quad (3)$$

with the rate equal to k_{sec}[2,6-AQDS]. The process includes also polarization transfer from polarized $NH_2-{}^{\bullet}CH_2$ radicals to 2,6-AQDS$^{\bullet-}$. From the kinetics of this secondary 2,6-AQDS$^{\bullet-}$ grow the second-order rate constant k_{sec} could be obtained, taking in account the spin−lattice relaxations of polarized radicals 2,6-AQDS$^{\bullet-}$ and $NH_2-{}^{\bullet}CH_2$ occurring on the same time scale. The measured time profiles have been simulated by using appropriated mathematical equations and necessary kinetic parameters,

most of them determined in this study (for details, see Discussion and Supporting Information). The resulting fits are shown as lines in Figure 10.

4. Discussion

From the overall rate constants for primary electron transfer reactions from the amino acids and some model compounds to the triplet excited 2,6-AQDS, as determined by experiments with optical detection, Table 2, several general conclusions could be derived. It has to be considered, that there are two main factors influencing the rate constants in the studied systems: (i) the standard reduction potential of the species/functional group to be oxidized and (ii) the electrostatic interaction in reactions with electrically charged donors (2,6-AQDS triplet is a double negative ion at all pHs used); the intensity of this factor depends on the actual ionic strength of the solution. Therefore, only the extrapolated $k_{q,0}$ values will be considered when electrically charged donors are discussed. It can be seen from Table 2 that α-amino acid anions, Gly^- and Ala^-, are reacting with the same rate constant of $k_{q,0} = 4.9 \times 10^8\ M^{-1}\ s^{-1}$ whereas β-Ala^- shows somewhat lower quenching ability (by a factor of approximately 2). The mechanism of the process is associated with the electron transfer from the nonbonding electron pair at nitrogen as the most probable site of attack. For glycine the standard reduction potential for the half reaction 4 is estimated to be 1.6 V[55] and a very similar value seems to apply to α-Ala^- and also β-Ala^-.

$$^{+\bullet}NH_2CH_2CO_2^- + e^- \rightarrow NH_2CH_2CO_2^- \quad (E^\circ = 1.6\ V) \quad (4)$$

$$NH_2CH_2CO_2^\bullet + e^- \rightarrow NH_2CH_2CO_2^- \quad (E^\circ = 2.3\ V) \quad (5)$$

$$^+NH_3CH_2CO_2^\bullet + e^- \rightarrow {}^+NH_3CH_2CO_2^- \quad (E^\circ = 2.9\ V) \quad (6)$$

Considerably higher rate constant for the same process (electron transfer from the primary amino group) found for methylamine in basic solutions, $k_q = 1.87 \times 10^9\ M^{-1}\ s^{-1}$, can easily be explained by the lower E° (1.3 V)[55] and the absence of the electrostatic repulsion in the interaction of 2,6-$AQDS_T$ dianion with this neutral molecule. Much higher energy is required, however, to abstract an electron from the carboxylate functional group. This is reflected in a considerably lower quenching rate constant observed for acetate anions, ($E^\circ = 2.1$ V[55]), $k_{q,0} = 0.44 \times 10^8\ M^{-1}\ s^{-1}$. Even lower rate constant should be assumed for the same process with α-amino acid anions because of the still somewhat higher E° value calculated for the corresponding half reaction 5. This allows the conclusion that in basic solutions a direct formation of amino acid acyloxyl radicals occurs with negligible probability. For amino acid zwitterions the carboxylate functional group is, however, the only site able to donate an electron. Because of the substantial increase of E° for the half reaction 6, the corresponding k_q values for $Gly^\pm$ and α-$Ala^\pm$ drop below the value observed for acetate anions despite the absence of any electrostatic repulsion in the case of zwitterions. The latter factor is probably responsible for the relatively high k_q value obtained for β-$Ala^\pm$, which is about three times higher than $k_{q,0}$ for acetate, although the two compounds should have very similar E°.

From the numerous literature[56] existing it is well-known that 2,6-AQDS triplet is a powerful oxidizing agent with the standard reduction potential of 2.37 V and is able to oxidize, for example, OH^- and Cl^- ($E^\circ(Cl/Cl^-) = 2.5$ V) with relatively high efficiency.[44] From the thermodynamic point of view the electron transfer reaction from the $Gly^\pm$ carboxylate group to 2,6-$AQDS_T$ is strongly endoergic. Despite this, $NH_2-{}^\bullet CH_2$ radicals have been found as the only product as determined by FT EPR measurements (Figure 1). It seems to us that the most probable precursor is the acyloxyl radical $^+NH_3CH_2CO_2^\bullet$ formed by the electron transfer mechanism as it is definitively the case with acetate (this work) and dipeptides in the zwitterionic form.[19] However, for the glycine zwitterions an alternative and kinetically not distinguishable pathway is possible. Namely, the H atom abstraction from the protonated amino group might occur as the primary quenching reaction, a pathway which might be energetically less demanding, eq 7. The resulting aminium radical would subsequently undergo fast decarboxylation.

SCHEME 2

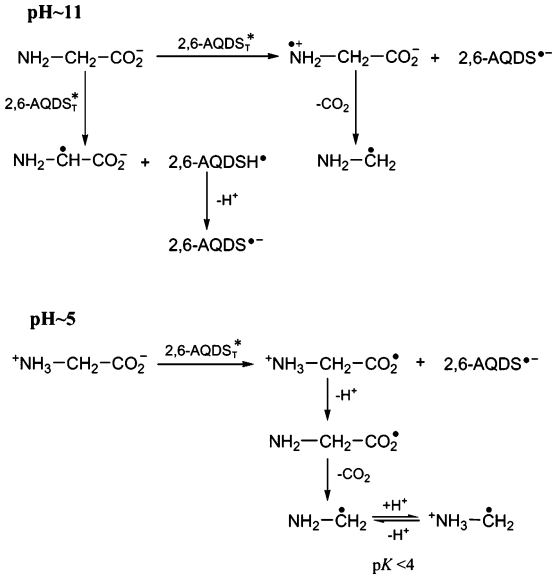

$$2,6\text{-}AQDS_T + {}^+NH_3-CH_2-CO_2^- \rightarrow 2,6\text{-}AQDSH^\bullet + {}^{+\bullet}NH_2-CH_2-CO_2^- \quad (7)$$

Arguments against reaction 7 are as follows: (i) although H atom abstraction from $Gly^\pm$ C−H bond should be energetically more favorable compared with N−H,[23] in acidic solutions no glycyl-type radicals (e.g., $NH_2-{}^\bullet CH-CO_2H$) have been detected; (ii) there has been no indication for H atom abstraction from the terminal $^+NH_3$- group in the case of β-$Ala^\pm$ (Figure 6) or Gly-$Gly^\pm$,[19] a reaction which would lead in both systems to characteristic products; (iii) the analysis of the EPR spectrum polarization pattern of the radical $NH_2-{}^\bullet CH_2$ strongly indicates that the aminium radical could be excluded as its precursor, see discussion below.

As already mentioned, primary radicals formed upon one-electron oxidation of all donors studied cannot be directly detected by ns time-resolved FT EPR measurements, most probably because of their very short lifetime. Under basic conditions the primary oxidation product of the α-amino acids studied is the aminium radical zwitterion which decays mainly by decarboxylation to generate the α-aminoalkyl radical $NH_2-{}^\bullet CR_2$ (Scheme 2). This unimolecular decarboxylation reaction takes place with a rate constant $k_{decarb} \cong 10^{11}\ s^{-1}$ as determined for α-aminoisobutyric acid.[14] With a yield of about 5% the α-amino-α-carboxylalkyl radical (glycyl-type radical) $NH_2-{}^\bullet CR-CO_2^-$ has also been detected for Gly^- and Ala^- (Figures 1 and 2). This radical may be generated by deprotonation of the aminium radical on the α-carbon position as a competition reaction channel to the decarboxylation as shown in Scheme 1.

It is interesting to note that no aminyl radical could be detected as a product for all three α-amino acid anions used as electron donors, although deprotonation of an aminium radical from the more acidic N−H position[57] should be more efficient. In fact, it has been shown in a recent pulse radiolysis study using hydroxyl radicals as oxidants[22] that only for N−H, but not C−H, the deprotonation of glycine aminium zwitterions radical can compete with the simultaneously occurring ultrafast decarboxylation. The same glycyl-type radicals could, however, be formed by another reaction pathway, occurring simultaneously to the electron transfer. This is the direct hydrogen atom abstraction from the α-carbon position by the 2,6-AQDS triplet as shown for glycine anion by eq 8 and in Scheme 2 (followed by a fast deprotonation of 2,6-AQDSH•, eq 9):

$$\text{2,6-AQDS}_T + \text{NH}_2-\text{CH}_2-\text{CO}_2^- \rightarrow \text{2,6-AQDSH}^\bullet + \text{NH}_2-{}^\bullet\text{CH}-\text{CO}_2^- \quad (8)$$

$$\text{2,6-AQDSH}^\bullet \rightarrow \text{2,6-AQDS}^{\bullet-} + \text{H}^+ \quad (9)$$

α-Aminoalkyl radicals have been detected as a low yield product also in other systems where NH_2- group is the main site of oxidative attack (NH_2-CH_3, β-Ala^-). Primary aminium radicals of both compounds, $^+{}^\bullet NH_2-CH_3$ and $^+{}^\bullet NH_2-CH_2-CH_2-CO_2^-$, deprotonate predominantly at nitrogen into aminyl radicals which have been detected as the main products (Figures 5 and 7). Because of relatively low dissociation energy of C−H bonds at α-amino position, a direct H atom abstraction seems to be the probable mechanism of $NH_2-{}^\bullet CH_2$ and $NH_2-{}^\bullet CH-CH_2-CO_2^-$ radicals formation in the case of NH_2-CH_3 and β-Ala^-, respectively, and also for the glycyl-type radicals for α-amino acid anions as shown by eq 8. It should be mentioned to this end that 2,6-AQDS triplet reacts with 2-propanol, a compound having the same α-C−H BDE as methylamine[22,58,59] and similar to other amino group containing compounds examined here,[22] by H atom abstraction mechanism with a quenching rate constants of 6×10^7 M^{-1} s^{-1}.[44,46] This allows us to conclude that such reaction could occur with a few percent probability in competition with the electron-transfer mechanism.

At pH 5, glycine is in a zwitterionic state with a protonated amino group and an unprotonated carboxyl group ($pK_a(R-CO_2H) = 2.34$). Therefore, the oxidation can take place only at the carboxylate site yielding the acyloxyl radical, $^+NH_3-CH_2-CO_2^\bullet$, as the primary oxidation product. The experimental observed $NH_2-{}^\bullet CH_2$ radical is generated by its subsequent fast decarboxylation reaction followed by the protonation equilibrium $^+NH_3-{}^\bullet CH_2/NH_2-{}^\bullet CH_2$ ($pK_a < 4$) as shown in Scheme 2. Analogous behavior has been observed for α-alanine and α-aminoisobutyric acid zwitterions. Their resulting α-aminoalkyl radicals show, however, remarkably higher pK_a values by at least two pH units in comparison with $^+NH_3-{}^\bullet CH_2$. Electron transfer from $-CO_2^-$ functional group to 2,6-$AQDS_T$ occurs also with β-$Ala^\pm$ and acetate anions as quenchers, followed by the fast decarboxylation via so-called Kolbe mechanism ($k = 10^9$ s^{-1} for $CH_3-CO_2^\bullet$ in methanol)[60] of their acyloxyl radicals into the respective alkyl radicals, Figures 6 and 8. In the case of β-$Ala^\pm$ this is the β-aminoethyl radical. The state of the amino group protonation of this radical could not be experimentally resolved but it seems reasonable to assume $pK_a(^+NH_3-CH_2-{}^\bullet CH_2/NH_2-CH_2-{}^\bullet CH_2) > 7$ because of the β-amino to $-{}^\bullet CH_2$ structure. Oxidation mechanisms for $R-NH_2$ and $R-CO_2^-$ compounds are shown in Scheme 3 on the examples of β-Ala^- and β-$Ala^\pm$, respectively.

The polarization pattern of $NH_2-{}^\bullet CH_2$ derived from glycine in acidic systems differs from that at pH 11 by a pure (E/A) behavior without any contribution of the triplet polarization whereas the 2,6-AQDS radical anion shows a lower intensity triplet polarization also at acidic pH, Figure 1. The intensity of the emissive $2,6\text{-AQDS}^{\bullet-}$ signal was seen to increase with increasing glycine concentration, whereas the radical pair polarized intensity of $NH_2-{}^\bullet CH_2$ signals kept constant (results not shown). The absence of triplet polarization of $NH_2-{}^\bullet CH_2$ was valid up to glycine concentration of 2.5 M. On the other hand, theoretical considerations predict an equal triplet contribution of the overall polarization for both radicals formed upon primary electron transfer event. From this we conclude that the primarily formed $^+NH_3-CH_2-CO_2^\bullet$ radical must have lost its triplet polarization before the decarboxylation reaction takes place. In other words, it has to be that the acyloxyl radical lifetime is longer than its spin−lattice relaxation time. Generally, the spin−lattice relaxation times of oxygen centered radicals are short,[61−63] usually in the order of some nanoseconds, suggesting the acyloxyl radical lifetime could also be in the few nanosecond time range. It should be mentioned at this point that at pH of about 5−6 used in our experiments, the decarboxylating acyloxyl radicals formed upon α-amino acid zwitterions oxidation are probably not the primarily formed $^+NH_3-CR_2-CO_2^\bullet$ but their deprotonated form, $NH_2-CR_2-CO_2^\bullet$. Namely, because of low pK_a of such radicals, a value of -0.4 has been calculated for $^+NH_3-CH_2-CO_2^\bullet$,[55] the deprotonation reaction could be assumed to occur very fast. The observed different characteristics of polarization patterns strongly suggests that for α-amino acids their corresponding acyloxyl and aminium radicals are distinct forms and that decarboxylation of the aminium radical is not preceded by the intramolecular carboxylate-to-amino electron-transfer step. Recently, Gould et al.[64] have come to similar conclusions based on the kinetics measurements of a series of aniline carboxylates oxidative decarboxylation as a function of solvent polarity.

Finally, the polarization pattern analysis allows us now to discard reaction 7 and formation of glycine aminium radical zwitterions as a mechanism for glycine oxidation in acidic solutions. The aminium intermediate would, namely, lead to an E*/A polarized EPR spectrum of the successor radical $NH_2-{}^\bullet CH_2$. This is in opposite to the experimental finding.

The time profiles of the radical anion $2,6\text{-AQDS}^{\bullet-*}$ normalized signal intensity (cf. Figure 10) contain complex information about the primary electron and polarization transfer between the triplet state 2,6-$AQDS_T$* and glycine anions, the secondary transfer of electron and polarization from the α-aminoalkyl radicals $NH_2-{}^\bullet CH_2$ to 2,6-AQDS ground state and the spin−lattice relaxation of the triplet and both radicals, where these

SCHEME 3

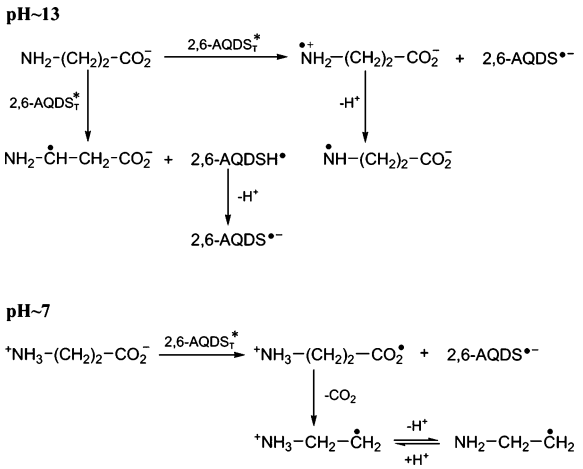

SCHEME 4

$$A_T^* \xrightarrow{T_{1T}} A_T \quad (10)$$

$$A_T^* \xrightarrow[k_q]{DB} A^{\bullet -*} + D^{\bullet *} + B^+ \quad (11)$$

$$A_T^* \xrightarrow{\tau_T} A_{S0} \quad (12)$$

$$D^{\bullet *} \xrightarrow{T_{1D}} D^{\bullet} \quad (13)$$

$$D^{\bullet *} \xrightarrow[k_{sec}]{A} A^{\bullet -*} + \text{products} \quad (14)$$

$$A^{\bullet -*} \xrightarrow{T_1} A^{\bullet -} \quad (15)$$

A = 2,6-AQDS, D = NH_2CH_2 or $NH_2CHCO_2^-$, B = CO_2^- or H

processes act in different time ranges. The primary electron transfer is finished after few nanoseconds already for the lowest glycine concentration used and the secondary reduction reaction is active in 100 ns to 2 μs. The spin−lattice relaxation processes are taking place on the nanosecond time scale for 2,6-AQDS$_T$* and with the time constant of about 1 and 10 μs for $NH_2-{}^{\bullet}CH_2$* and 2,6-AQDS$^{\bullet -*}$, respectively. Consequently, the spin−lattice relaxation of 2,6-AQDS$^{\bullet -*}$ dominates in 1 to 100 μs time scale (cf. Figure 10). Above 100 μs, the stable Boltzmann signal of 2,6-AQDS$^{\bullet -}$ is observed (the lifetime of 2,6-AQDS$^{\bullet -}$ is several milliseconds). This separation in time of the different processes simplifies the calculation of the polarization time profiles of 2,6-AQDS$^{\bullet -*}$ (see below). The reaction scheme describing chemical and physical (relaxation of spin polarization) changes taking place is given by the equations in Scheme 4. In eq 11, the primary electron transfer and the fast decarboxylation reaction and/or fast deprotonation of different primary radicals are collected because their time behavior cannot be resolved in our experiments. Under our experimental conditions the chemical changes can be assumed to occur in quantitative yields. The spin−lattice relaxation of the polarized radicals has to be, however, included in the mathematical description of 2,6-AQDS$^{\bullet -*}$ time profiles as they are occurring in competition to the polarization transfer processes (cf. Supporting Information). Polarization of 2,6-AQDS$^{\bullet -}$ induced by radical−radical interactions has been neglected. This assumption is justified if the spectral centers of the interacting radicals are nearly identical. Then the E/A polarizations originating from the radical pair mechanism of symmetrical lines from the spectral center have the same absolute values but different signs. That means, that the radical polarization is canceled in the intensity (integral over all lines) of 2,6-AQDS$^{\bullet -*}$. Under the assumption that the spin−lattice relaxation and the deactivation by electron transfer to the polarized triplet 2,6-AQDS$_T$* are independent processes, the time dependence of the normalized triplet magnetization $A_T(t)$ of 2,6-AQDS$_T$* can be represented by

$$A_T(t) = c_T(t) \times P_T(t) \quad (16)$$

where $c_T(t)$ denotes the triplet concentration and $P_T(t)$ the triplet polarization. For comparison with the experimental data $A_T(t)$ is normalized to the Boltzmann intensity of 2,6-AQDS$^{\bullet -}$ = $A_{eq}^{\bullet -}$. Both quantities were calculated by

$$dc_T/dt = -k_q c_T[DB] - c_T/\tau_T$$

$$dP_T/dt = -(P_T - P_T^{eq})/T_{1T} \quad (17)$$

where τ_T is the lifetime of the triplet in the absence of a donor (DB) at given pH, P_{T0} is the initial value $P_T(0)$ and P_T^{eq} is the Boltzmann polarization of the triplet. The result is given by

$$A_T(t) = ((P_{T0} - 4/3)\exp(-t/T_{1T}) + 4/3)\exp(-(k_q[DB] + 1/\tau_T)t) \quad (18)$$

This time dependence $A_T(t)$ is used to solve the kinetic equations for the primary and secondary generation of [2,6-AQDS$^{\bullet -*}$] = $A^{\bullet -}(t)$ described by the differential equations:

$$dA^{\bullet -}/dt = k_q A_T[DB] + k_{sec} D^{\bullet}[A] - (A^{\bullet -} - A_{eq}^{\bullet -})/T_1$$

$$dD^{\bullet}/dt = k_q A_T[DB] - k_{sec} D^{\bullet}[A] - (D^{\bullet} - D_{eq}^{\bullet})/T_{1D} \quad (19)$$

The analytical solution is given in the Supporting Information by a simple, but long formula used to simulate the measured normalized signal intensity−time profiles of 2,6-AQDS$^{\bullet -*}$. The formula contains six parameters: P_{T0} the initial polarization of the triplet, T_{1T} the spin−lattice relaxation time of the polarized triplet, k_q the rate constant of the primary electron transfer, k_{sec} the rate constant of the secondary reduction of 2,6-AQDS by D$^{\bullet}$*, T_1 the spin−lattice relaxation time of 2,6-AQDS$^{\bullet -*}$ and T_{1D} the spin−lattice relaxation time of the polarized radical D$^{\bullet}$*. For the simulations of time profiles measured for three different [DB] as shown in Figure 10, the same parameters were taken. They were deduced from experiments with optical detection (k_q and τ_T, see section 3.5) and from the comparison with experiments using methylamine as electron donor (T_{1T}). The free parameters were k_{sec}, P_{T0}, and T_{1D}. Because of the complete conversion of D$^{\bullet}$ to A$^{\bullet -}$, the Boltzmann intensity was normalized to $A_{eq}^{\bullet -} = 2$. The results of simulations are shown with the solid lines in Figure 10, and the numerical values of known parameters and those obtained by simulations are given in Table 3. For the free parameters, the best fit of all three time profiles has been obtained by using $P_{T0} = -53$. $k_{sec} = 3 \times 10^9$ M^{-1} s^{-1}, a value in very good agreement with 2.6×10^9 M^{-1} s^{-1} reported for the reduction of 2,6-AQDS with the similar radical $NH_2-{}^{\bullet}CH-CO_2^-$;[65] $T_{1D} = 1.5$ μs, an acceptable and reasonable value for the spin−lattice relaxation time for this type of C-centered radicals.[66;67] The good fit of the experimental results in Figure 10 with glycine as electron donor confirm the proposed reaction mechanism and the method of analysis.

5. Conclusions

Photooxidation of simple aliphatic α-amino acids by the triplet state of anthraquinone-2,6-disulfonate in aqueous solution results in their degradation into CO_2 and corresponding α-aminoalkyl radicals irrespective of pH ≥ 3, i.e., so long amino acids are in the zwitterionic or anionic protonation form. Reductive electron transfer is always the major primary mechanism. The deprotonated amino group is the preferential site of attack leading to the formation of aminium radicals as short living precursors. Electron transfer from the carboxylic functional group and formation of acyloxyl radical intermediates occurs with at least 10 times lower rate constants and is therefore operative only for amino acid zwitterions. Both primary transients, aminium and acyloxyl radicals, undergo fast one step fragmentation into the same products, CO_2 and α-aminoalkyl radicals, but they do not constitute resonance mesomeric forms

TABLE 3: Fit Parameters of the 2,6-AQDS$^{\bullet-}$ Time Profiles from Figure 10[a]

parameter	Gly$^-$ concentration/mM		
	50	75	100
$k_q \times [Gly^-]/\mu s^{-1}$	75	112.5	150
$k_{sec} \times [2,6\text{-AQDS}]/\mu s^{-1}$	1.5	1.5	1.5
T_{1T}/ns	1.6	1.6	1.6
$T_1/\mu s$	10	10	10
$T_{1D}/\mu s$	1.5	1.5	1.5
P_{T0}	−53	−53	−53
$\tau_T/\mu s$	0.2	0.2	0.2
$A_{eq}^{\bullet-}$	2	2	2

[a] For explanation see text.

of one and the same species. This is concluded from the polarization pattern analysis of the successor α-aminoalkyl radicals, the first FT EPR detectable products on 100 ns time scale. Whereas aminium precursor leads to the triplet and radical pair polarized α-aminoalkyl radicals, only radical pair polarization could be detected for the same radicals produced over the acyloxyl route. This strongly indicates that the acyloxyl radical, with the unpaired electron located on oxygen, is considerably longer living species (by about 3 orders of magnitude) than the aminium radical, losing its triplet polarization by spin−lattice relaxation before undergoing decarboxylation.

Acknowledgment. This work was supported in part by the Deutsche Forschungsgemeinschaft and Graduiertenkolleg "Mechanisms and Applications of Non-Conventional Oxidation Reactions" at the University of Leipzig.

Supporting Information Available: Text discussing the mathematical description of the intensity time profiles. This material is available free of charge via the Internet at http://pubs.acs.org.

References and Notes

(1) Beckman, K. B.; Ames, B. N. *Physiol. Rev.* **1998**, *78*, 547.
(2) Davies, M. J. *BBA-Proteins Proteomics* **2005**, *1703*, 93.
(3) Stadtman, E. R. *Annu. Rev. Biochem.* **1993**, *62*, 797.
(4) Neta, P.; Fessenden, R. W. *J. Phys. Chem.* **1971**, *75*, 738.
(5) Paul, H.; Fischer, H. *Helv. Chim. Acta* **1971**, *54*, 485.
(6) Riesz, P.; Rustgi, S. N. *Radiat. Phys. Chem.* **1979**, *13*, 21.
(7) Armstrong, D. A.; Hemmerich, P.; Traber, R. *Photochem. Photobiol.* **1982**, *21*, 747.
(8) Heeslis, P. F. *Chem. Soc. Rev.* **1982**, *11*, 15.
(9) Mönig, J.; Chapman, R.; Asmus, K.-D. *J. Phys. Chem.* **1985**, *89*, 3139.
(10) Su, Z.; Mariano, P. S.; Falvey, D. E.; Yoon, U. C.; Oh, S. W. *J. Am. Chem. Soc.* **1998**, *120*, 10676.
(11) Bonifačić, M.; Štefanić, I.; Hug, G. L.; Armstrong, D. A.; Asmus, K.-D. *J. Am. Chem. Soc.* **1998**, *120*, 9930.
(12) Canle-Lopez, M.; Santaballa, J. A.; Steenken, S. *Chem.—Eur. J.* **1999**, *5*, 1192.
(13) Bonifačić, M.; Armstrong, D. A.; Carmichael, I.; Asmus, K.-D. *J. Phys. Chem. B* **2000**, *104*, 643.
(14) Hug, G. L.; Bonifačić, M.; Asmus, K.-D.; Armstrong, D. A. *J. Phys. Chem. B* **2000**, *104*, 6674.
(15) Hug, G. L.; Fessenden, R. W. *J. Phys. Chem. A* **2000**, *104*, 7021.
(16) Lü, J. M.; Wu, L. M.; Geimer, J.; Beckert, D. *Phys. Chem. Chem. Phys.* **2001**, *3*, 2053.
(17) Štefanić, I.; Bonifačić, M.; Asmus, K.-D.; Armstrong, D. A. *J. Phys. Chem. A* **2001**, *105*, 8681.
(18) Wisniowski, P.; Carmichael, I.; Fessenden, R. W.; Hug, G. L. *J. Phys. Chem. A* **2002**, *106*, 4573.
(19) Tarábek, P.; Bonifačić, M.; Naumov, S.; Beckert, D. *J. Phys. Chem. A* **2004**, *108*, 929 and Tarábek, P.; Bonifačić, M.; Beckert, D. *J. Phys. Chem. A* **2004**, *108*, 3467.
(20) Nunome, K.; Muto, H.; Toriyama, K.; Iwasaki, M. *J. Chem. Phys.* **1976**, *65*, 3805.
(21) Sinclair, J. *J. Chem. Phys.* **1971**, *55*, 245.
(22) Armstrong, D. A.; Asmus, K.-D.; Bonifačić, M. *J. Phys. Chem. A* **2004**, *108*, 2238.
(23) Yu, D.; Rauk, A.; Armstrong, D. A. *J. Am. Chem. Soc.* **1995**, *117*, 1789.
(24) Lü, J. M.; Geimer, J.; Naumov, S.; Beckert, D. *Phys. Chem. Chem. Phys.* **2001**, *3*, 952.
(25) Geimer, J.; Hildenbrand, K.; Naumov, S.; Beckert, D. *Phys. Chem. Chem. Phys.* **2000**, *2*, 4199.
(26) Geimer, J.; Beckert, D. *J. Phys. Chem. A* **1999**, *103*, 3991.
(27) Geimer, J.; Brede, O.; Beckert, D. *Chem. Phys. Lett.* **1997**, *276*, 411.
(28) Bowman, M. K. in *Modern Pulsed and Continuous-wave Electron Spin Resonance*; Kevan, L., Bowman, M. K., Eds.; J. Wiley & Sons: New York, 1990; pp 1−42.
(29) Bowman, M. K.; Toporowicz, M.; Norris, J. R.; Michalski, T. J.; Angerhofer, A.; Levanon, H. *Isr. J. Chem.* **1988**, *28*, 215.
(30) Freed, J. H. *Annu. Rev. Phys. Chem.* **2000**, *51*, 655.
(31) Gorcester, J.; Millhauser, G. L.; Freed, J. H. In *Advanced EPR, Applications in Biology and Biochemistry*; Hoff, A. J., Ed.; Elsevier: Amsterdam, 1989; pp 177−242.
(32) Kroll, G.; Plüschau, M.; Dinse, K. P.; van Willigen, H. *J. Chem. Phys.* **1990**, *93*, 8709.
(33) Beckert, D. In *Electron paramagnetic resonance*; Gilbert, B. C., Davies, M. J., Murphy, D. M., Eds.; Specialist Periodical Reports 18; Royal Society of Chemistry: Cambridge, U.K., 2002; pp 74−108.
(34) Freed, J. H.; Pedersen, J. B. *Adv. Magn. Reson.* **1976**, *8*, 1−80.
(35) Steiner, U. E.; Ulrich, T. *Chem. Rev.* **1989**, *89*, 51.
(36) McLauchlan, K. A. *J. Chem. Soc., Perkin Trans. 2* **1997**, 2465.
(37) Adeleke, B. B.; Wan, J. K. S. *J. Chem. Soc., Faraday Trans. 1* **1976**, 1799.
(38) Atkins, P. W.; Evans, G. T. *Mol. Phys.* **1974**, *27*, 1633.
(39) Monchick, L.; Adrian, F. J. *J. Chem. Phys.* **1978**, *68*, 4376.
(40) Adrian, F. J. *J. Chem. Phys.* **1972**, *57*, 5107.
(41) Muus, L. T.; Atkins, P. W.; McLauchlan, K. A.; Pedersen, J. B. *Chemical Induced Magnetic Polarization*, D. Reidel Publ.: Dordrecht, The Netherlands, 1977.
(42) Säuberlich, J. Ph.D. Dissertation, University of Leipzig, 1996.
(43) Murov, S. L.; Carmichael, I.; Hug, G. L. *Handbook of Photochemistry*; Marcel Dekker Inc.: New York, Basel, Switzerland, and Hong Kong, 1993.
(44) Loeff, I.; Rabani, J.; Treinin, A.; Linschitz, H. *J. Am. Chem. Soc.* **1993**, *115*, 8933.
(45) Säuberlich, J.; Brede, O.; Beckert, D. *J. Phys. Chem. A* **1997**, *101*, 5659.
(46) Kausche, T.; Säuberlich, J.; Trobitzsch, E.; Beckert, D.; Dinse, K. P. *Chem. Phys.* **1996**, *208*, 375.
(47) Stephenson, D. S. *Nucl. Magn. Reson. Spectrosc.* **1988**, *20*, 515.
(48) Geimer, J.; Beckert, D. *Appl. Magn. Reson.* **2000**, *18*, 505.
(49) Symons, M. C. R. *J. Chem. Soc., Perkin Trans. 2* **1973**, 97.
(50) Davies, M. J.; Gilbert, B. C.; Norman, R. O. C. *J. Chem. Soc., Perkin Trans. 2* **1984**, 503.
(51) Loeff, I.; Treinin, A.; Linschitz, H. *J. Phys. Chem.* **1984**, *88*, 4931 and Loeff, I.; Treinin, A.; Linschitz, H. *J. Phys. Chem.* **1983**, *87*, 2536.
(52) Values published earlier for quenching of 2,6-AQDS$_T$ with amino acid anions, including Gly$^-$ and Ala$^-$,[16] and OH$^-$ [44,53] were measured under undefined and not constant ionic strength and are therefore not recommendable.
(53) Moore, J. N.; Phillips, D.; Nakashima, N.; Yoshihara, K. *J. Chem. Soc., Faraday Trans. 2* **1986**, *82*, 745.
(54) Wardman, P. *J. Phys. Chem. Ref. Data* **1989**, *18*, 1637.
(55) Armstrong, D. A.; Rauk, A.; Yu, D. *J. Chem. Soc., Perkin Trans. 2* **1995**, 553.
(56) Mukherjee, T. Radiation chemistry of quinones. In *Radiation Chemistry: Present Status and Future Trends*; Jonah, C. D., Rao, B. S. M., Eds.; Elsevier Science B. V.: Amsterdam, 2001; p 287.
(57) Yoon, U. C.; Mariano, P. S. *Adv. Electron-Transfer Chem.* **1994**, *4*, 117.
(58) Bonifačić, M.; Armstrong, D. A.; Štefanić, I.; Asmus, K.-D. *J. Phys. Chem. B* **2003**, *107*, 7268.
(59) Wayner, D. D. M.; Clark, K. B.; Rauk, A.; Yu, D.; Armstrong, D. A. *J. Am. Chem. Soc.* **1997**, *119*, 8925.
(60) Hilborn, J. W.; Pincock, J. A. *J. Am. Chem. Soc.* **1991**, *113*, 2683.
(61) Fessenden, R. W. *J. Chem. Phys.* **1973**, *58*, 2489.
(62) Verma, N. C.; Fessenden, R. W. *J. Chem. Phys.* **1973**, *58*, 2501.
(63) Trifunac, A. D.; Avery, E. C. *Chem. Phys. Lett.* **1974**, *27*, 141.
(64) Gould, I. R.; Lenhard, J. R.; Farid, S. *J. Phys. Chem. A* **2004**, *108*, 10949.
(65) Rao, P. S.; Hayon, E. *Nature (London)* **1973**, *243*, 344.
(66) Fessenden, R. W.; Hornak, J. P.; Venkataraman, B. *J. Chem. Phys.* **1981**, *74*, 3694.
(67) Poole, C. P.; Farach, H. A. *Handbook of Electron Spin Resonance*; Am. Inst. Phys.: New York, 1994.